

Effects of Al_2O_3 support modifications on MoO_x and VO_x catalysts for dimethyl ether oxidation to formaldehyde

Haichao Liu, Patricia Cheung and Enrique Iglesia*

Department of Chemical Engineering, University of California at Berkeley, Berkeley, CA 94720, USA. E-mail: iglesia@cchem.berkeley.edu; Fax: (510) 642-4778; Tel: (510) 642-9673

Received 10th March 2003, Accepted 21st July 2003

First published as an Advance Article on the web 31st July 2003

Dispersed two-dimensional MoO_x and VO_x oligomers on Al_2O_3 and SnO_x -modified Al_2O_3 supports were examined for selective dimethyl ether (DME) oxidation to HCHO and their structure and reduction rates in H_2 were determined using Raman and X-ray near edge absorption spectroscopies (XANES), respectively. Modifying Al_2O_3 supports with SnO_x or other reducible oxides (ZrO_x , CeO_x and FeO_x) led to MoO_x domains with higher rates for catalytic DME oxidation and for reduction in H_2 , while maintaining the high HCHO selectivity observed on $\text{MoO}_x/\text{Al}_2\text{O}_3$ catalysts. This appears to reflect the higher reactivity of lattice oxygen atoms as Mo-O-M acquires more reducible M cations. On Al_2O_3 modified with SnO_x species at near monolayer coverages (5.5 Sn nm^{-2}) DME oxidation turnover rates (per Mo-atom) were approximately three times greater than on unmodified Al_2O_3 samples containing predominately polymolybdate domains ($\sim 7 \text{ Mo nm}^{-2}$). The rates of DME oxidation and of reduction by H_2 increased in parallel with increasing Sn surface density, but they were significantly higher than on MoO_x domains supported on bulk crystalline SnO_2 . The use of more reducible VO_x domains instead of MoO_x also led to higher DME oxidation rates (per V or Mo atom) without significant changes in HCHO selectivity and to effects of Al_2O_3 modification by SnO_x similar to those observed on MoO_x -based catalysts. Al_2O_3 supports with higher surface area led to catalytic materials with similar rates per V or Mo atom and similar HCHO selectivities for a given surface density ($\sim 7 \text{ V or Mo nm}^{-2}$), because of the prevalence of accessible two-dimensional oligomeric domains of the active oxides on both Al_2O_3 supports at these surface densities. Higher surface area Al_2O_3 supports, however, led to proportionately higher rates per catalyst mass, as a result of the larger number of active domains that can be accommodated at higher surface areas. These studies provide a rationale for the design of more efficient catalysts for selective DME oxidation to HCHO and illustrate the significant catalytic productivity improvements available from support modifications in oxidation catalysts.

1. Introduction

Formaldehyde (HCHO) is produced *via* methanol (CH_3OH) oxidation and widely used as an intermediate in the synthesis of many chemicals.¹ Recent advances in dimethyl ether (DME, CH_3OCH_3) synthesis from H_2/CO reactants make DME an attractive precursor for HCHO and for other chemicals currently produced from CH_3OH .^{2–4} The selective oxidation of dimethyl ether on catalysts based on dispersed MoO_x and VO_x structures provides an alternate and selective route for HCHO synthesis at low temperatures.⁵

Recently, we have shown that small MoO_x domains consisting predominately of two-dimensional polymolybdate structures supported on Al_2O_3 , ZrO_2 and SnO_2 catalyze DME oxidation with high primary HCHO selectivities (80–98% HCHO, CH_3OH -free basis) and high reaction rates⁵ at much lower temperatures than previously reported.^{6–10} MoO_x domains supported on SnO_2 showed the highest DME oxidation turnover rates, but relatively low HCHO selectivities, while similar MoO_x domains supported on Al_2O_3 gave very high HCHO selectivities, but lower oxidation turnover rates.^{5,11}

DME oxidation to HCHO occurs *via* redox cycles involving lattice oxygen atoms.¹² DME oxidation turnover rates increase in parallel with increasing rates of the stoichiometric reduction of MoO_x domains using H_2 as the reductant; larger domains and more reducible supports led to higher rates

for both DME oxidation and MoO_x reduction with H_2 .^{11,13} Kinetic studies have probed the primary and secondary reactions responsible for the observed HCHO selectivities during DME oxidation, which depend also on the domain size and on the nature of the underlying supports. Less reducible supports with higher Lewis acidity led to the weaker binding of DME-derived intermediates and of HCHO on Mo^{6+} sites, which favor HCHO desorption and discourage HCHO readorption and secondary reactions to form CO_x and methyl formate.^{11,13}

These significant effects of active oxide reducibility and of support identity on turnover rates and HCHO selectivities led us to tailor the reduction properties of active MoO_x domains by modifying Al_2O_3 supports, which exhibited low turnover rates and high HCHO selectivities, with a surface coating of a more reducible oxide before anchoring MoO_x domains. We report here a detailed study of DME conversion to HCHO on MoO_x and VO_x domains supported on Al_2O_3 modified with SnO_x , ZrO_x , CeO_x and FeO_x overlayers, and also of the structure and reduction properties of the active oxide domains. We also explore additional improvements in catalytic reaction rates by coating Al_2O_3 supports of higher surface areas. In doing so, this study provides useful details for the rational design of selective catalysts for the conversion of DME to HCHO and also reports catalytic materials with unprecedented reactivity and selectivity for this reaction.

2. Experimental

2.1 Synthesis of catalytic materials

SnO_x-modified Al₂O₃ supports (SnO_x-Al₂O₃ and ZrO_x-Al₂O₃) were prepared by incipient wetness impregnation of Al₂O₃ (Degussa, AG, 101 m² g⁻¹, or Alcoa, HiQ31, 196 m² g⁻¹; designated as Al₂O₃(A) and Al₂O₃(B), respectively) with an isopropanol solution of Sn(i-C₃H₇O)₄ (Alfa Aesar, 98% metal basis) at 298 K. Impregnated samples were kept in dry N₂ for 5 h at 298 K, and then dried at 393 K in ambient air overnight and treated in flowing dry air (Airgas, zero grade) at 673 K for 3 h. ZrO_x, CeO_x and FeO_x-modified Al₂O₃ supports (ZrO_x-Al₂O₃, CeO_x-Al₂O₃ and FeO_x-Al₂O₃) were prepared by incipient wetness impregnation of Al₂O₃(A) (Degussa, AG, 101 m² g⁻¹) with aqueous solutions of ZrO(NO₃)₂ (Aldrich, 99.99%), Ce(NO₃)₄ (Aldrich, 99.99%) and Fe(NO₃)₃·9H₂O (Aldrich, 99.99%), respectively, at 298 K for 5 h in ambient air. Impregnated samples were then dried at 393 K in ambient air overnight and treated in flowing dry air (Airgas, zero grade) at 673 K for 3 h. SnO₂ was prepared by hydrolysis of an aqueous tin(IV) chloride pentahydrate (98%, Alfa Aesar) solution at a pH of ~7 using NH₄OH (14.8 M, Fisher Scientific). The precipitates were washed with deionized water until the effluent was free of Cl ions, as detected by AgNO₃ addition. The resulting solids were treated in flowing dry air (Airgas, zero grade) at 773 K for 3 h.

Supported MoO_x catalysts were prepared by incipient wetness impregnation of these supports with aqueous (NH₄)₆-Mo₇O₂₄ (Aldrich, 99%) solutions. Supported VO_x catalysts were similarly prepared using aqueous ammonium metavanadate [NH₄VO₃] (Aldrich, 99%) solutions containing oxalic acid (Mallinckrodt, analytical grade; NH₄VO₃-oxalic acid (0.5 M)). All samples were dried at 393 K in ambient air overnight after impregnation and treated in flowing dry air (Airgas, zero grade) at 773 K for 3 h. The Mo or V surface density for all supported samples is reported as Mo nm⁻² or V nm⁻², based on the Mo or V content determined from the concentration of the impregnating solution and the BET total surface area for each sample.

2.2 Structural characterization

Surface areas were measured using N₂ at its normal boiling point (Autosorb-1; Quantachrome) and BET analysis methods. Raman spectra were measured at 298 K in ambient air using a HoloLab 5000 Raman spectrometer (Kaiser Optical) and a frequency-doubled Nd:YAG laser at a wavelength of 532 nm. Samples were pressed into self-supporting thin wafers and placed on a rotary stage within a quartz cell. The samples were rotated at 16 Hz in order to avoid structural damage from local laser heating.

2.2 Reducibility of supported MoO_x samples in H₂

The rates of stoichiometric reduction of MoO_x in H₂ were measured using *in situ* Mo-K edge X-ray absorption near-edge spectroscopy (XANES). XANES spectra were measured using beamline 4-1 at the Stanford Synchrotron Radiation Laboratory. The electron storage ring was operated at 3.0 GeV with a beam current of 82 mA. Samples were diluted with Al₂O₃ in order to maintain a constant concentration of Mo absorbers (5 wt%) in all samples and then pressed and sieved to retain 0.18–0.25 mm particles. These particles were placed in a quartz capillary (1.0 mm OD, 0.1 mm wall thickness) held horizontally in a heated chamber.¹⁴ The sample was treated at 773 K for 1 h in flowing 20% O₂-He (~0.1 cm³ s⁻¹; Airgas, certified mixture), cooled to ambient temperature in He, and heated to 823 K at 0.167 K s⁻¹ in flowing 20% H₂-Ar (~0.1 cm³ s⁻¹; Matheson UHP, certified mixture).

A Si (111) crystal monochromator was used and detuned by 30% in order to eliminate the harmonics. The spectra were measured in transmission mode using 5 eV increments in the pre-edge region (19.905–19.990 keV), 0.50 eV increments in the near-edge region (19.990–20.033 keV) and 0.04 Å⁻¹ in the fine structure region (20.033–20.200 keV). Each XANES spectrum consists of a single scan at the energy increments. Energies were calibrated by placing the first inflection point of a Mo foil held in the beam path at its reported absorption energy (19.999 keV). Spectra were analyzed using WinXAS (Version 1.2).¹⁵ Background subtraction was carried out using a linear fit of the pre-edge region and a cubic spline for the post-edge region. The fraction of the Mo present as Mo⁴⁺ was determined from the 19.990–20.180 keV spectral region using linear superimposition methods¹⁶ and the spectra of MoO₂ and of each unreduced catalyst sample.

2.3 Catalytic reactions of dimethyl ether

Dimethyl ether oxidation reaction rates and selectivities were measured at 513 K in a packed-bed quartz flow reactor. Catalyst samples (0.15–0.30 g) were diluted with acid-washed quartz powder (~1 g) in order to prevent bed temperature gradients and treated in flowing 20% O₂-He (0.67 cm³ s⁻¹) for 1.5 h at 773 K before catalytic measurements. The reactant mixture consisted of 80 kPa DME (99.5%, Praxair), 18 kPa O₂ and 2 kPa N₂ (2 kPa) (Praxair, Certified O₂-N₂ mixture). Homogeneous reactions were detected in empty reactors only above 590 K.

The reactants and products in the effluent stream were analyzed by on-line gas chromatography (Hewlett-Packard 6890 GC) using a methyl silicone capillary column (HP-1; 30 m, 0.25 mm, 0.25 μm film) and a Porapak Q packed column (80–100 mesh, 1.82 m, 3.18 mm) connected to flame ionization and thermal conductivity detectors, respectively. Methanol, formaldehyde (HCHO), methyl formate (MF), CO, CO₂, H₂O, and trace amount of dimethoxymethane (DMM) were the only products detected.

Dimethyl ether conversions were varied by changing the reactant space velocity and kept below 10% in all experiments. DME reaction rates and product selectivities were extrapolated to zero residence time in order to obtain the corresponding primary rates and selectivities. In view of the available pathways for DME-CH₃OH interconversion and for CH₃OH conversion to HCHO, rates and selectivities are reported here on a methanol-free basis.^{11,13}

3. Results and discussion

Previous studies^{11,13} on the effects of support and of the reducibility of active oxide domains on the rate and selectivity of DME oxidation reactions led us to prepare and evaluate Al₂O₃ supports modified with more reducible oxides, in an attempt to increase reaction rates without the loss of HCHO selectivity that previously accompanied the use of more reducible bulk oxides as supports. Our initial approach involved chemical modifications of Al₂O₃ surfaces with well-dispersed SnO_x species; SnO_x was chosen because it led to very high activity and reducibility for MoO_x domains, albeit with significant selectivity to undesired CO_x (CO + CO₂) by-products in previous studies.¹¹

Fig. 1 shows primary DME conversion rates and primary selectivities to HCHO, methyl formate (MF), and CO_x (CO + CO₂) on samples with Mo surface densities of ~7 Mo nm⁻² as the SnO_x surface density varies from zero to 11.2 Sn nm⁻² on Al₂O₃(A). Al₂O₃(A) and SnO_x-modified Al₂O₃(A) did not catalyze DME reactions at these conditions in the absence of active MoO_x species. Primary HCHO selectivities remained nearly unchanged on MoO_x/Al₂O₃(A) (~98%)

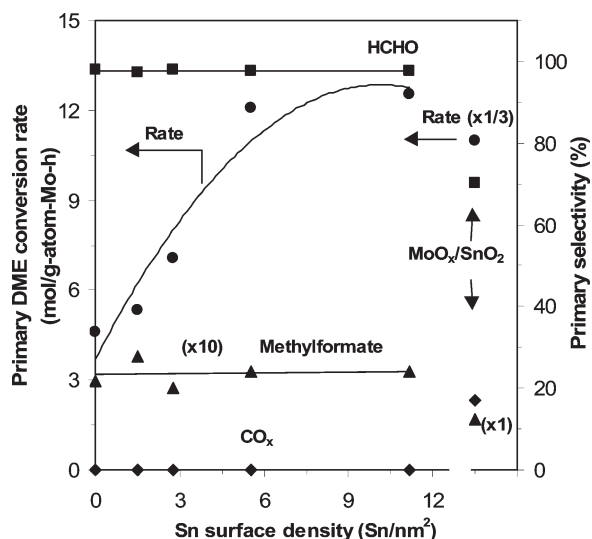


Fig. 1 Primary DME conversion rates and primary selectivities to HCHO, methyl formate (MF) and CO_x ($\text{CO} + \text{CO}_2$) as a function of Sn surface density on $\text{MoO}_x/\text{SnO}_x\text{-Al}_2\text{O}_3(\text{A})$ catalysts at Mo surface densities of $\sim 7.0 \text{ Mo nm}^{-2}$ (513 K; 80 kPa DME, 18 kPa O_2 and 2 kPa N_2).

within this Sn surface density range. Primary MF ($\sim 2\%$) selectivities were very low and CO_x was not detected on these samples.

Raman and X-ray absorption spectra, as well as the absence of X-ray diffraction lines (not shown here), showed that MoO_x species exist predominately as two-dimensional polymolybdate domains on these samples. As a result, most MoO_x species reside at surfaces and they are accessible for catalytic DME reactions; therefore measured reaction rates (per Mo) become turnover rates and reflect the reactivity of exposed surfaces on polymolybdate domains. These turnover rates increased from 4.6 to 12.8 mol (g-atom Mo h) $^{-1}$ as Sn surface densities on $\text{Al}_2\text{O}_3(\text{A})$ increased from 0 to 11.2 Sn nm $^{-2}$. These rates (per Mo) remained below those measured on polymolybdate domains supported on bulk crystalline SnO_2 (32.6 mol (g-atom Mo h) $^{-1}$, Fig. 1, Table 1). Thus, it appears that the formation of more reducible MoO_x species as SnO_x increasingly covers Al_2O_3 supports leads in turn to faster redox cycles during DME oxidation turnovers to HCHO.¹² The formation of Mo–O–Sn linkages between dispersed MoO_x domains and $\text{SnO}_x\text{-Al}_2\text{O}_3(\text{A})$ or SnO_2 surfaces leads to an apparent increase in electron density at lattice oxygen atoms compared with that in Mo–O–Al structures prevalent on pure Al_2O_3 surfaces. This proposal was confirmed by the parallel increase in the rate of stoichiometric reduction of MoO_x domains in H_2 observed with increasing Sn surface density.

In SnO_x -containing samples, some concurrent reduction of MoO_x and SnO_x species prevents the use of H_2 consumption

rates to measure the rate of incipient reduction of Mo^{6+} species to defect oxides.¹¹ *In-situ* X-ray absorption spectroscopy near the Mo–K edge (XANES), however, is an element-specific technique that allows direct measurements of the extent of reduction of MoO_x domains. The concentrations of Mo^{6+} and Mo^{4+} were estimated by linear superimposition methods using the starting spectrum and the spectrum for crystalline MoO_2 as principal components.

Fig. 2 shows the Mo–K near-edge spectra for MoO_x (7.1 Mo nm^{-2}) supported on $\text{Al}_2\text{O}_3(\text{A})$ modified with a monolayer of SnO_2 (5.5 Sn nm^{-2} ; $\text{MoO}_x/\text{SnO}_2\text{-Al}_2\text{O}_3(\text{A})$) during contact with 20% $\text{H}_2\text{-Ar}$ at 298, 623, 723 and 823 K, and for crystalline MoO_2 at ambient conditions. The pre-edge feature weakened with increasing temperature and the spectral features approached those typical of crystalline MoO_2 . Above 623 K, the spectra are accurately described by linear combinations of the spectra for the initial sample (at 298 K) and for crystalline MoO_2 , without any spectral contribution from crystalline MoO_3 or any other species.

Fig. 3 shows the fraction of the Mo atoms present as Mo^{4+} as the sample temperature increases in 20% $\text{H}_2\text{-Ar}$ for MoO_x domains ($\sim 7.0 \text{ Mo nm}^{-2}$) on $\text{Al}_2\text{O}_3(\text{A})$ modified with various amounts of SnO_x . At each temperature, the Mo^{4+} fraction increased with increasing Sn surface density and it was highest on bulk crystalline SnO_2 . Thus, we conclude that the replacement of Mo–O–Al prevalent in $\text{MoO}_x/\text{Al}_2\text{O}_3$ with Mo–O–Sn linkages leads to more reactive oxygen atoms and to more reducible Mo cations, as also inferred from the effects of SnO_2 modification on catalytic DME oxidation rates (Fig. 1 and Table 1). These data provide additional evidence for the mechanistic connection between the catalytic and the redox properties of oxide domains in DME oxidation reaction,^{11,13} as also found for other reactions involving redox cycles, such as oxidative dehydrogenation of alkanes^{16,17} and of alcohols.^{18,19} These findings are consistent with the involvement of lattice oxygen atoms and with kinetically-relevant steps involving C–H bond activation in adsorbed methoxide species, which require transition states leading to electron donation to metal centers during catalytic cycles leading to HCHO synthesis from DME.¹²

DME oxidation reactions occur *via* parallel and sequential steps shown in Scheme 1;¹³ these steps include primary DME reactions to form CH_3OH (k_0), HCHO (k_1), methyl formate (MF) (k_2) and CO_x (k_3), as well as secondary reactions of primary HCHO products to form MF (k_4) and CO_x (k_5).¹³ HCHO selectivities depend on two rate constant ratios, $k_1/(k_2 + k_3)$ and $k_1/((k_4 + k_5)C_{\text{Ao}})$, where k_i is the reaction rate constant for reaction i and C_{Ao} the inlet DME concentration.¹³ Values of $k_1/(k_2 + k_3)$ reflect primary DME conversion rates to HCHO (k_1) relative to those for MF (k_2) and CO_x (k_3) formation; thus, they provide an alternate measure of primary HCHO selectivities. In contrast, $k_1/((k_4 + k_5)C_{\text{Ao}})$ ratios reflect primary HCHO formation rates (k_1) relative to the rates for secondary HCHO reactions to form MF (k_4) and CO_x (k_5); this kinetic parameter reflects the relative

Table 1 Primary DME conversion rates, selectivities and relative rate constants for MoO_x domains supported on unmodified $\text{Al}_2\text{O}_3(\text{A})$ and SnO_2 and on $\text{Al}_2\text{O}_3(\text{A})$ modified with near one monolayer SnO_x , ZrO_x , CeO_x and FeO_x (513 K; 80.0 kPa DME, 18 kPa O_2 and 2 kPa N_2)

Catalyst (MoO_x wt%)	Mo surface density/ Mo nm^{-2}	Primary DME reaction rate/ $\text{mol (g-atom Mo h)}^{-1}$	Primary selectivity (%)				
			HCHO	MF	CO_x	$k_1/(k_2 + k_3)$	$k_1/((k_4 + k_5)C_{\text{Ao}})$
$\text{MoO}_x/\text{Al}_2\text{O}_3(\text{A})$ (15.0%)	7.0	4.6	98.1	1.9	0	45	0.35
$\text{MoO}_x/\text{SnO}_2$ (5.9%)	6.3	32.6	70.4	12.5	17.2	2.4	0.08
$\text{MoO}_x/\text{SnO}_x\text{-Al}_2\text{O}_3(\text{A})$ (15.0%)	7.1	12.2	97.7	2.3	0	43	0.31
$\text{MoO}_x/\text{ZrO}_x\text{-Al}_2\text{O}_3(\text{A})$ (15.0%)	6.8	8.7	98.6	1.4	0	70	0.27
$\text{MoO}_x/\text{CeO}_x\text{-Al}_2\text{O}_3(\text{A})$ (13.4%)	6.6	6.8	98.8	1.2	0	82	0.29
$\text{MoO}_x/\text{FeO}_x\text{-Al}_2\text{O}_3(\text{A})$ (14.9%)	6.9	6.2	99.7	0.3	0	332	0.29

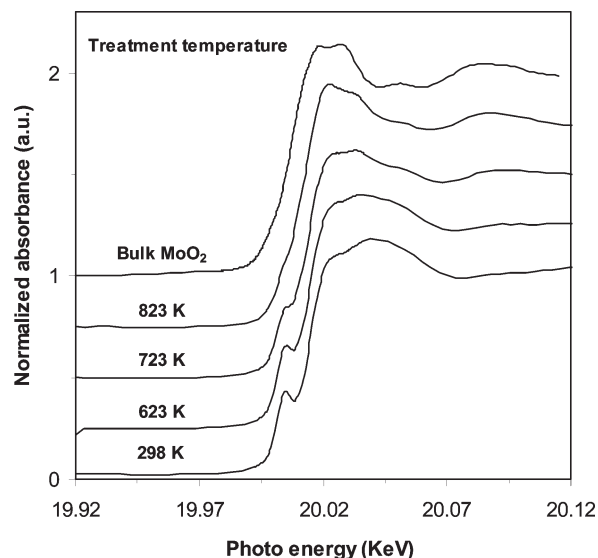


Fig. 2 X-Ray absorption spectra near the Mo K edge for $\text{MoO}_x/\text{SnO}_2\text{-Al}_2\text{O}_3$ (A) (7.1 Mo nm^{-2} ; 5.5 Sn nm^{-2}) after treatment in H_2 (20% $\text{H}_2\text{-Ar}$) at 298, 623, 723 and 823 K and for crystalline MoO_2 at ambient temperature.

tendency of a given catalyst to form and convert HCHO. Higher values of $k_1/(k_2 + k_3)$ and $k_1/((k_4 + k_5)C_{\text{Ao}})$ lead to higher HCHO selectivities at a given DME conversion and the latter becomes increasingly important as DME conversion increases in determining HCHO yields.

Fig. 4 shows $k_1/(k_2 + k_3)$ and $k_1/((k_4 + k_5)C_{\text{Ao}})$ values as a function of Sn surface density. The $k_1/(k_2 + k_3)$ ratios remained nearly constant as Sn surface density increased from zero to 11.2 Sn nm^{-2} , consistent with the previously discussed constant primary HCHO selectivities (Fig. 1). The $k_1/((k_4 + k_5)C_{\text{Ao}})$ ratios, however, initially remained similar to those on pure Al_2O_3 supports, but then decreased for Sn surface densities greater than 5.5 Sn nm^{-2} . These Sn surface density effects indicate that near-monolayer SnO_x coverages ($\sim 5.0 \text{ Sn nm}^{-2}$, for $\text{SnO}_2(110)$ planes) on Al_2O_3 provide a compromise between the higher reactivity of MoO_x domains supported on SnO_x -modified Al_2O_3 and the HCHO yield

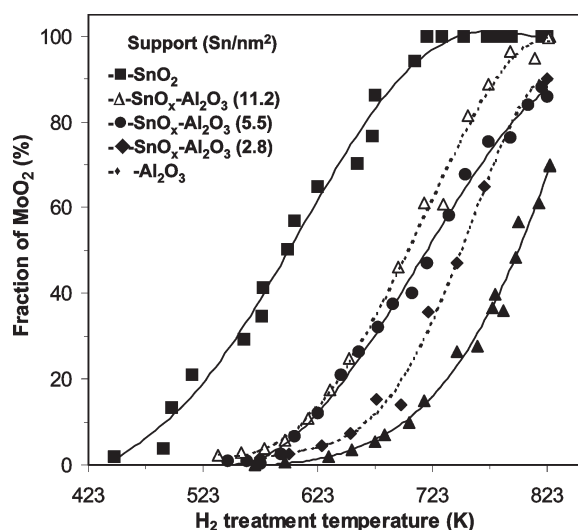
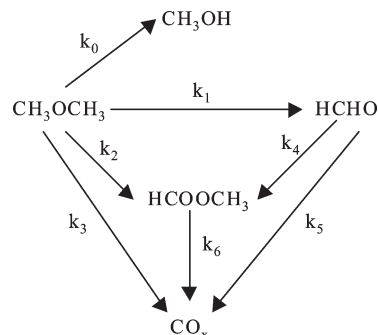


Fig. 3 MoO_2 fraction measured from linear superimposition of MoO_2 and initial spectra as a function of treatment temperature in 20% $\text{H}_2\text{-Ar}$ for MoO_x domains supported on SnO_x -modified $\text{Al}_2\text{O}_3(\text{A})$ with Sn surface densities of 2.8 (\diamond), 5.5 (\bullet) and $11.2 (\triangle) \text{ Sn nm}^{-2}$, and on unmodified $\text{Al}_2\text{O}_3(\text{A})$ (\blacktriangle) and SnO_2 (\blacksquare) at similar Mo surface density ($6.3\text{--}7.1 \text{ Mo nm}^{-2}$).



Scheme 1 Primary and secondary reaction pathways for dimethyl ether conversion on MoO_x -based catalysts.

losses that prevail as SnO_2 crystallites form at higher Sn surface densities. Chemical modifications of Al_2O_3 with near monolayer coverages of ZrO_2 , CeO_2 and Fe_2O_3 also led to higher DME conversion rates compared with $\text{MoO}_x/\text{Al}_2\text{O}_3$ ($\sim 7 \text{ Mo nm}^{-2}$) (Table 1), without significant changes in primary or secondary HCHO selectivities (see $k_1/((k_4 + k_5)C_{\text{Ao}})$ values in Table 1).

Clearly, the catalytic function of polymolybdate domains depends on the chemical identity and the reduction properties of the support surfaces to which they are atomically connected. These effects appear to be reasonably general and to apply also to oxidation reactions of DME on VO_x domains. Polyvanadate domains are more reducible than polymolybdate domains on a given support surface,¹⁶ and modifications of Al_2O_3 supports with SnO_x (5.5 Sn nm^{-2}) lead to higher DME oxidation rates (per active metal atom). Table 2 shows that DME oxidation rates (per active metal atom) on $\text{VO}_x/\text{Al}_2\text{O}_3(\text{A})$ and $\text{VO}_x/\text{SnO}_x\text{-Al}_2\text{O}_3(\text{A})$ were 1.5 and 1.4 times greater than for MoO_x domains on each respective support. Primary HCHO selectivities and $k_1/(k_2 + k_3)$ ratios, as well as $k_1/((k_4 + k_5)C_{\text{Ao}})$ ratios on these VO_x catalysts were similar to those measured on MoO_x domains for a given support. As for MoO_x domains, chemical modifications of $\text{Al}_2\text{O}_3(\text{A})$ by a monolayer of SnO_x led to an increase in the DME conversion rate by a factor of 2.4 on VO_x samples. For WO_x domains, which are less reducible than MoO_x and VO_x domains,¹⁷ DME conversion products were not detected on either $\text{WO}_x/\text{Al}_2\text{O}_3(\text{A})$ (7.6 W nm^{-2}) or $\text{WO}_x/\text{SnO}_x\text{-Al}_2\text{O}_3(\text{A})$ (7.8 W nm^{-2}) at reaction temperatures between 513 and 553 K.

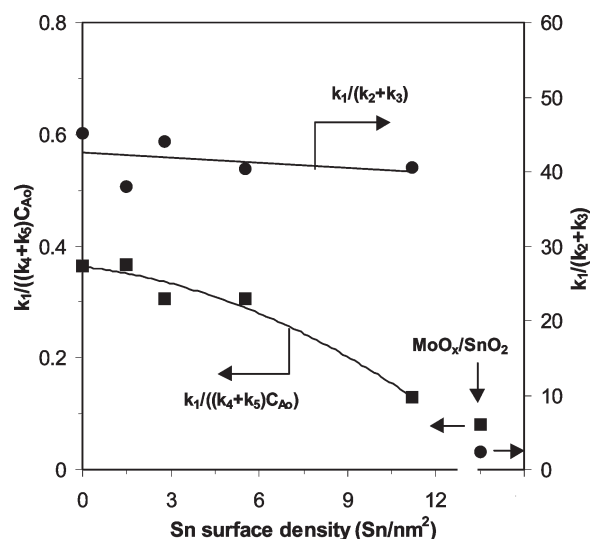


Fig. 4 Rate constant ratios $k_1/(k_2 + k_3)$ and $k_1/((k_4 + k_5)C_{\text{Ao}})$ as a function of Sn surface density on $\text{MoO}_x/\text{SnO}_x\text{-Al}_2\text{O}_3(\text{A})$ catalysts at Mo surface densities of $\sim 7.0 \text{ Mo nm}^{-2}$ (513 K; 80 kPa DME, 18 kPa O_2 and 2 kPa N_2).

Table 2 Primary DME conversion rates, selectivities and relative rate constants on MoO_x, VO_x and WO_x domains at near one monolayer surface density supported on unmodified and SnO_x-modified Al₂O₃(A) (5.5 Sn nm⁻²) (513 K; 80.0 kPa DME, 18 kPa O₂ and 2 kPa N₂)

Catalyst (MO _x wt%)	M surface density/ Metal nm ⁻²	Primary DME reaction rate/ mol (g-atom Mo h) ⁻¹	Primary selectivity (%)				
			HCHO	MF	CO _x	$k_1/(k_2 + k_3)$	$k_1/((k_4 + k_5)C_{AO})$
MoO _x /Al ₂ O ₃ (A) (15.0%)	7.0	4.6	98.1	1.9	0	45	0.35
VO _x /Al ₂ O ₃ (A) (10.0%)	8.0	6.8	99.5	0.5	0	199	0.29
WO _x /Al ₂ O ₃ (A) (18.0%)	7.6	0	–	–	–	–	–
MoO _x /SnO _x -Al ₂ O ₃ (A) (15.0%)	7.1	12.2	97.7	2.3	0	43	0.31
VO _x /SnO _x -Al ₂ O ₃ (A) (10.1%)	7.9	16.3	97.7	2.3	0	43	0.27
WO _x /SnO _x -Al ₂ O ₃ (A) (16.8%)	7.8	0	–	–	–	–	–

Next, we explored whether practical rates per catalyst mass (or volume) can be improved by using modified Al₂O₃ supports with higher surface area and anchoring well-dispersed MoO_x or VO_x domains at surface densities corresponding to near monolayer coverages. In effect, we attempt here to simply increase the number of active sites, while maintaining the support composition (SnO_x-Al₂O₃; 5.5 Sn nm⁻²) and the active oxide surface densities (~ 7 Mo nm⁻² or ~ 8 V nm⁻²) that led to highest site reactivities on modified alumina supports with lower surface area. We examined the structure and catalytic properties of four samples: MoO_x and VO_x supported on Al₂O₃(B) and SnO_x-Al₂O₃(B), both of which have higher surface areas (196 and 181 m² g⁻¹, respectively) than the corresponding pure and SnO_x-modified Al₂O₃(A) materials discussed above (Tables 3 and 4).

Fig. 5 shows Raman spectra in the 500–1100 cm⁻¹ range for MoO_x/Al₂O₃(B), MoO_x/Al₂O₃(A), MoO_x/SnO_x-Al₂O₃(B) and MoO_x/SnO_x-Al₂O₃(A) samples with similar surface densities (6.4–7.1 Mo nm⁻²). MoO_x/Al₂O₃(B) (6.4 Mo nm⁻²) showed a broad band at ~ 965 cm⁻¹ and a shoulder at ~ 912 cm⁻¹, which are assigned to terminal Mo=O and bridging Mo–O–Mo stretching modes in two-dimensional oligomeric MoO_x, respectively.^{16,20} This sample also showed three sharper bands at 674, 825 and 1003 cm⁻¹, characteristic of crystalline MoO₃.²⁰ The strong MoO₃ bands in this sample suggest the presence of some crystalline MoO₃, but Raman scattering cross-sections are 10–10³ times greater for MoO₃ than for dispersed MoO_x species.^{21,22} Thus, we conclude from the observed relative intensities for the 965 and the 1003 cm⁻¹ bands that this sample contains predominately two-dimensional MoO_x oligomers. This conclusion was confirmed by the absence of MoO₃ X-ray diffraction lines and by the lack of MoO₃ features in the X-ray absorption fine structure spectra for this sample. These Raman features are similar to those observed in MoO_x/Al₂O₃(A) (7.0 Mo nm⁻²), which has a lower surface area, but similar Mo surface densities as MoO_x/Al₂O₃(B) (6.4 Mo nm⁻²); thus, MoO_x domains are structurally similar on the two Al₂O₃ supports, as long as surface densities are kept relatively constant. The two SnO_x-modified samples, MoO_x/SnO_x-Al₂O₃(B) (6.4 Mo nm⁻²) and MoO_x/SnO_x-Al₂O₃(A) (7.1 Mo nm⁻²), also showed simi-

lar Raman features, and two bands were detected at ~ 965 cm⁻¹ and ~ 912 cm⁻¹, showing the two-dimensional MoO_x oligomers present on the support surfaces at the similar Mo surface densities.

Table 3 shows primary DME reaction rates and HCHO selectivities, as well as the two kinetic parameters responsible for selectivities [$k_1/(k_2 + k_3)$ and $k_1/((k_4 + k_5)C_{AO})$] at 513 K on these four MoO_x catalyst samples. On MoO_x domains supported on pure Al₂O₃, DME reaction rates per gram of catalyst increased from 4.7 to 9.4 mmol (g-cat h)⁻¹ as the sample surface area increased from 90.0 to 174.9 m² g⁻¹, indicating a proportional increase in catalyst productivity with increasing surface area. Reaction rates per Mo-atom (4.7 vs. 5.1 mmol (g-atom Mo h)⁻¹), primary HCHO selectivities (98.1 vs. 96.0%) and $k_1/(k_2 + k_3)$ (45 vs. 31) and $k_1/((k_4 + k_5)C_{AO})$ (0.35 vs. 0.31) ratios were very similar on these two samples; these results confirm that the dispersion and structure of MoO_x are unaffected by the surface area of the Al₂O₃ support, as long as Mo surface densities are kept at similar values. Similarly, DME conversion rates per gram of catalyst on MoO_x/SnO_x-Al₂O₃(B) (6.4 Mo nm⁻²) and MoO_x/SnO_x-Al₂O₃(A) (7.1 Mo nm⁻²) were nearly proportional to their surface area and no significant changes in primary or secondary HCHO selectivities were detected (Table 3).

VO_x-based catalysts showed similar trends. Table 4 shows that DME reaction rates increased with increasing support surface area for VO_x species supported at similar surface densities on Al₂O₃[VO_x/Al₂O₃(B) (7.8 V nm⁻²) and VO_x/Al₂O₃(A) (8.0 V nm⁻²)] and SnO_x-Al₂O₃ [VO_x/SnO_x-Al₂O₃(B) (7.5 V nm⁻²) and VO_x/SnO_x-Al₂O₃(A) (7.9 V nm⁻²)] supports. Site reactivities (DME oxidation rates per V-atom) and HCHO selectivity parameters were unaffected by changes in the surface area of the support; we note also that the site reactivity enhancements introduced by SnO_x overlayers are maintained on the higher surface area Al₂O₃ supports. Thus, catalyst productivities can be significantly improved by exploiting the beneficial effects of SnO_x overlayers and of well-dispersed polymolybdate domains on alumina supports with higher surface areas, while maintaining near monolayer surface densities for both the SnO_x modifier and the active MoO_x or VO_x domains.

Table 3 Surface area effects on primary DME conversion rates, HCHO selectivities and relative rate constants for MoO_x domains at near one monolayer surface density supported on unmodified and SnO_x-modified Al₂O₃ (~ 5.5 Sn nm⁻²) (513 K; 80.0 kPa DME, 18 kPa O₂ and 2 kPa N₂)

Support (MoO _x wt%)	BET surface area/m ² g-cat	Mo surface density/ Mo nm ⁻²	Primary DME reaction rate/ mmol (g-cat h) ⁻¹	Primary DME reaction rate/mol (g-atom Mo h) ⁻¹	Primary HCHO selectivity (%)	$k_1/(k_2 + k_3)$	$k_1/((k_4 + k_5)C_{AO})$
Al ₂ O ₃ (A) (15.0%)	90.0	7.0	4.7	4.6	98.1	45	0.35
Al ₂ O ₃ (B) (26.8%)	174.7	6.4	9.4	5.1	95.9	23	0.32
SnO ₂ -Al ₂ O ₃ (A) (15.0%)	87.9	7.1	12.6	12.1	97.7	41	0.31
SnO ₂ -Al ₂ O ₃ (B) (22.9%)	150.3	6.4	18.4	11.4	98.2	55	0.41

Table 4 Surface area effects on primary DME conversion rates, HCHO selectivities and relative rate constants for VO_x domains at near one monolayer surface density supported on unmodified and SnO_x-modified Al₂O₃ (~5.5 Sn nm⁻²) (513 K; 80.0 kPa DME, 18 kPa O₂ and 2 kPa N₂)

Support (V ₂ O ₅ wt%)	BET surface area/m ² (g-cat) ⁻¹	V surface density/V nm ⁻²	Primary DME reaction rate/mmol (g-cat h) ⁻¹	Primary DME reaction rate/mol (g-atom V h) ⁻¹	Primary HCHO selectivity (%)	$k_1/(k_2 + k_3)$	$k_1/((k_4 + k_5)C_{AO})$
Al ₂ O ₃ (A) (10.0%)	83.0	8.0	6.7	6.8	99.5	199	0.29
Al ₂ O ₃ (B) (23.2%)	195.9	7.8	13.5	5.9	97.1	34	0.30
SnO ₂ -Al ₂ O ₃ (A) (10.1%)	84.3	7.9	16.2	16.3	97.7	43	0.27
SnO ₂ -Al ₂ O ₃ (B) (16.8%)	149.2	7.5	25.3	15.3	98.0	52	0.28

4. Conclusions

Improvements of the reactivity of the supported MoO_x domains, without significant loss of the selective properties of the Al₂O₃-supported MoO_x catalyst for DME conversion to HCHO, were achieved by surface modification of Al₂O₃ supports with reducible SnO_x, ZrO_x, CeO_x and FeO_x, as a result of the increase in the reducibility of the MoO_x domains on the modified Al₂O₃ supports. SnO_x is the best modifier among these oxides. The reducibility and reactivity of the supported MoO_x domains on SnO_x-Al₂O₃ supports increase in parallel with increasing the Sn surface density, and a monolayer coverage of SnO_x species provides the best compromise between the reactivity and the selectivity properties of the supported MoO_x domains. At 5.5 Sn nm⁻², near one monolayer coverage, the DME oxidation rate (per Mo atom) is about three times greater for MoO_x/SnO_x-Al₂O₃ than the rate for unmodified MoO_x/Al₂O₃ at similar Mo surface densities of ~7.0 Mo nm⁻². Replacing MoO_x species by more reducible VO_x species also leads to higher DME oxidation rates (per Mo or V atom) without significant changes in HCHO selectivity (as reflected by the $k_1/(k_2 + k_3)$ and $k_1/((k_4 + k_5)C_{AO})$ ratios) and to effects of Al₂O₃ modification by SnO_x similar to those observed on MoO_x-based catalysts. Al₂O₃ supports with higher surface area led to catalytic materials with similar rates per V or Mo atom and similar HCHO selectivities for a given surface density (~7 V or Mo nm⁻²), because of the prevalent presence of accessible two-dimensional oligomeric

domains of the active oxides on both Al₂O₃ supports at these surface densities. Higher surface area Al₂O₃ supports lead to proportionately higher rates per catalyst mass, as a result of the larger number of active domains that can be accommodated at higher surface areas.

Acknowledgements

This study was supported by BP as part of the Methane Conversion Cooperative Research Program at the University of California at Berkeley. The authors also acknowledge helpful technical discussions with Drs Theo Fleisch and John Collins of BP. The X-ray absorption data were collected at Stanford Synchrotron Radiation Laboratory (SSRL), which is operated by Department of Energy (DOE), Office of Basic Energy Sciences under contract DE-AC03-76SF00515.

References

- J. M. Tatibouet, *Appl. Catal., A*, 1997, **148**, 213.
- J.-L. Li, X.-G. Zhang and T. Inui, *Appl. Catal. A*, 1996, **147**, 23.
- T. H. Fleisch, A. Basu, M. J. Gradassi and J. G. Masin, *Stud. Surf. Sci. Catal.*, 1997, **107**, 117.
- T. Shikada, Y. Ohno, T. Ogawa, M. Ono, M. Mizuguchi, K. Tomura and K. Fujimoto, *Stud. Surf. Sci. Catal.*, 1998, **119**, 515.
- H. Liu and E. Iglesia, *J. Catal.*, 2002, **208**, 1.
- G. P. Hagen and M. J. Spangler, *US Pat.*, 6,265,528, 2001.
- G. P. Hagen and M. J. Spangler, *US Pat.*, 6,350,919, 2002.
- R. M. Lewis, R. C. Ryan and L. H. Slaugh, *US Pat.* 4,442,307, 1984.
- R. M. Lewis, R. C. Ryan and L. H. Slaugh, *US Pat.*, 4,439,624, 1984.
- R. M. Lewis, R. C. Ryan and L. H. Slaugh, *US Pat.*, 4,435,602, 1984.
- H. Liu, P. Cheung and E. Iglesia, *J. Catal.*, 2003, **217**, 222.
- H. Liu, P. Cheung and E. Iglesia, unpublished results.
- H. Liu, P. Cheung and E. Iglesia, *J. Phys. Chem. B*, 2003, **107**, 4118.
- W. Li, G. D. Meitzner, R. W. Borry III and E. Iglesia, *J. Catal.*, 2000, **191**, 373.
- T. Ressler, *WinXAS 97*, version 1.2, 1998.
- K. Chen, S. Xie, A. T. Bell and E. Iglesia, *J. Catal.*, 2001, **198**, 232.
- K. Chen, A. T. Bell and E. Iglesia, *J. Catal.*, 2002, **209**, 35.
- G. Deo and I. E. Wachs, *J. Catal.*, 1994, **146**, 323.
- W. Zhang, A. Desikan and S. T. Oyama, *J. Phys. Chem.*, 1995, **99**, 14468.
- G. Mestl and T. K. K. Srinivasan, *Catal. Rev.-Sci. Eng.*, 1998, **38**, 451.
- R. Radhakrishnan, C. Reed, S. T. Oyama, M. Semen, J. N. Kondo, K. Domen, Y. Ohminami and K. Asakura, *J. Phys. Chem. B*, 2001, **105**, 8519.
- C. C. Williams, J. G. Ekerdt, J. M. Jehng, F. D. Hardcastle and I. E. Wachs, *J. Phys. Chem.*, 1991, **95**, 9791.

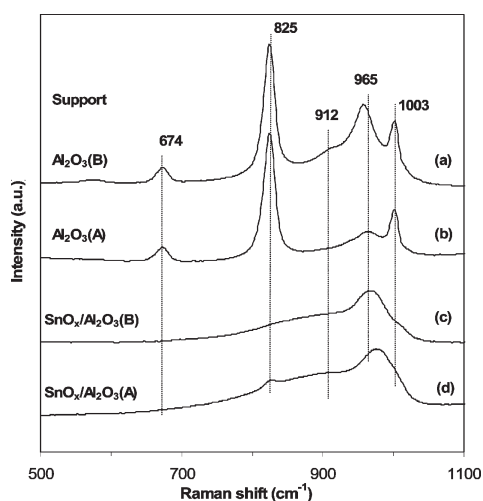


Fig. 5 Raman spectra for (a) MoO_x/Al₂O₃(B), (b) MoO_x/Al₂O₃(A), (c) MoO_x/SnO_x-Al₂O₃(B) and (d) MoO_x/SnO_x-Al₂O₃(A) catalysts with surface densities of 6.4–7.1 Mo nm⁻² at ambient conditions.